PHYSICAL REVIEW B **90**, 235407 (2014)

Stable structure of high In coverage on Si(111)-α-$\sqrt{3} \times \sqrt{3}$-Au

Shih-Yu Wu,[1] Chia-Hsiu Hsu,[1] Wang-chi V. Yeh,[2] Hsin Lin,[3] Feng-Chuan Chuang,[1] and Chien-Cheng Kuo[1,*]
[1] *Department of Physics, National Sun Yat-sen University, Kaohsiung 80424, Taiwan*
[2] *Department of Physics, National Dong Hwa University, Hualien 97401, Taiwan*
[3] *Department of Physics, National University of Singapore, Singapore 117542, Singapore*

(Received 18 July 2014; revised manuscript received 13 November 2014; published 2 December 2014)

The structure of 0.8 ML In coverage on the Si(111)-$\sqrt{3} \times \sqrt{3}$-Au surface is investigated by scanning tunneling microscopy/spectroscopy and low energy electron diffraction. By depositing 1.2 ML In at room temperature followed by annealing at 500 °C, the surface reveals the $\sqrt{7} \times \sqrt{3}$ structure with 0.8 ML In coverage. The detailed atomic structure is studied by both the topography and dI/dV images, and the results are further supported by the density functional theory. The observed structure has higher In coverage than the previous experiments and has not been proposed in the previous calculations.

DOI: 10.1103/PhysRevB.90.235407 PACS number(s): 68.35.−p, 68.37.Ef, 68.55.Nq, 73.20.−r

I. INTRODUCTION

As one of the most intensively studied systems, the metallic overlayer on Si(111) has provided a playground for a wide variety of surface science studies in the past few decades [1]. It has attracted a great deal of attention due to its unique electronic properties in one and two dimensions [2–8]. One famous example of these properties is the two-dimensional electron gas (2DEG) behavior for the $\sqrt{3} \times \sqrt{3}$ structure ($\sqrt{3}$ hereafter) of the Au overlayer on Si(111) [9–11]. In this case, the electronic structure is sensitive to the Au coverage due to its complicated domain wall structures. It was demonstrated that a domain walls free structure can be obtained by adsorbing a small amount (0.15–0.5 ML) of In with a subsequently short annealing at 600 °C [12]. This homogeneous surface sharpens the free electron surface band of the α-$\sqrt{3}$ Au overlayer, which then possesses the properties of a perfect isotropic 2DEG system [13].

Moreover, the In atoms act as electron donors that would cause the surface conduction bands to shift down by 200–500 meV. One may wonder if the band structures and chemical potential of this system can be further modulated by depositing more In on the surface. Experimentally, the energy shift seems to have no systematic dependence on the In coverage. Manipulating the surface bands is not likely to be achieved by increasing the In coverage due to the stable 0.15 ML $\sqrt{3} \times \sqrt{3}$ In structure on Si(111)-α-$\sqrt{3}$-Au [13]. The deposition of additional In atoms develops three-dimensional islands but not the surface structure with higher In coverage [12]. Theoretically, the possibility of a surface structure with higher In coverage, which is energetically favorable over the bare $\sqrt{3} \times \sqrt{3}$-Au surface, was proposed recently based on the density functional theory (DFT) [14]. The surface structure with higher In coverage is of interest as it shows the Rashba spin-orbit splitting from the calculations. Furthermore, previous experimental results of the In surface structure show the higher transition temperature of two dimensional superconducting states for higher In coverage [15–17]. It is thus imperative to find the stable structure of In with higher coverage on Si(111)-α-$\sqrt{3}$-Au.

In this work, we found the order structure with higher In coverage can be stabilized on Si(111)-α-$\sqrt{3}$-Au. By using scanning tunneling microscopy/spectroscopy (STM/STS) and low energy electron diffraction (LEED), we observed a $\sqrt{7} \times \sqrt{3}$ In at 0.8 ML on Si(111)-α-$\sqrt{3}$-Au. The detailed atomic model of the 0.8 ML In structure was constructed by comparing the atomically resolved STM, dI/dV images, and the DFT calculations.

II. EXPERIMENTAL AND CALCULATION DETAILS

The experiments were performed in an ultrahigh vacuum (3×10^{-10} torr) system equipped with STM/STS and LEED. Clean Si(111) 7 × 7 surfaces were prepared by outgasing at 600 °C for 6 h followed by flashing at around 1200 °C. The In deposition rate was 0.02 ML/min, calibrated by the well known $\sqrt{3} \times \sqrt{3}$ phase of In on Si(111), of which the coverage is known to be 0.3 ML as compared to the 1 × 1 unit cell of Si(111) [9,18,19]. The Au deposition rate was calibrated by observing the α-$\sqrt{3}$ Au structure on Si(111) [20]. The deposition of Au on Si(111) was initially held at ∼ 500 °C and then the temperature was slowly cooled down to room temperature. The annealing temperature was estimated by the power-temperature relation which was measured by a thermocouple fixed at a test sample. The estimated error for the temperature is ±10 °C by the fluctuation of the heating power as the sample dimension varies slightly from sample to sample. The system was prepared by deposition of In on the Si(111)-α-$\sqrt{3}$-Au surface at RT and followed by annealing at 500 °C for 2 min. Low energy electron diffraction was taken at RT for the structure confirmation. STM measurements were done with a tungsten tip at RT and 78 K. STS was acquired simultaneously with the topography at 78 K only for better stability. The dI/dV spectra were normalized by dividing the tunneling probability T to compare with the local density of states (LDOS) from the theory [21].

The calculations [22–24] were performed within the generalized gradient approximation using projector-augmented-wave potentials [25], as implemented in the Vienna Ab-Initio Simulation Package (VASP) [26,27]. The bulk Si was constructed from a periodically repeating slab consisting of

---

[*] Author to whom correspondence should be addressed: cckuo@faculty.nsysu.edu.tw

three Si bilayers, a reconstructed layer, and a vacuum space of 12 Å. Hydrogen atoms were used to passivate the Si dangling bonds at the bottom of the slab. The position of these hydrogen atoms and the Si atoms of the bottom bilayer were kept fixed at the bulk crystalline positions. The proposed models, including In, Au, and remaining Si atoms, were relaxed till the residual force was smaller than 0.01 eV/Å. Other relevant parameters can be found in our previous study [14]. The simulated STM images were carried out by Tersff-Hamann approximation for the proposed models [28]. The calculated LDOS were the DOS of all states attributed only from the topmost In layer.

III. RESULTS AND DISCUSSION

Figure 1 comprises the topological and structural information for the Si(111)-α-$\sqrt{3}$-Au as well as the In overlayer on top of it. Figure 1(a) shows the atomic terraces with clear domain wall structure for the Si(111)-α-$\sqrt{3}$-Au surface, which agrees with the previous STM results [20,29,30]. A sharp LEED pattern with the typical $\sqrt{3}\times\sqrt{3}$-$R30^\circ$ superstructure confirms the homogeneity of this surface [9,10], as shown in Fig. 1(b). After depositing 1.2 ML In on this surface at RT, clusters are formed, as shown in Fig. 1(c). The formation of clusters was observed in the previous study after depositing more than 0.2 ML In [12]. These clusters become smaller in a postannealing procedure at 400 °C [Fig. 1(d)] and disappear at higher temperatures, say 500 °C [Fig. 1(e)]. Alternatively, the surface becomes flat with terraces decorated with the two-dimensional islands. The height of the islands is 3.16 ± 0.05 Å and changes slightly (~0.1 Å) with bias. In contrast to the original $\sqrt{3}\times\sqrt{3}$ superstructure, a clear $\sqrt{7}\times\sqrt{3}$ domain shows up, as depicted in Fig. 1(f), which agrees with the simulated LEED pattern of the $\sqrt{7}\times\sqrt{3}$ with three domains [31]. In addition, a $\sqrt{7}\times\sqrt{3}$ superstructure, which was never observed, forms on the topmost surface. Several annealing temperatures were tested and no other clear LEED patterns were found for temperatures below 500 °C. Note that the domain wall structure of α-$\sqrt{3}$-Au was not observed on the terraces nor on the decorated islands, which indicates that a complete and structure-homogeneous overlayer is formed. The homogeneity of the surface was also confirmed by the similar STS features at different positions on the surface. As the height of the islands (3.16 Å) is close to the Si step height (3.14 Å), the observed islands are likely due to the different Si layers underneath. This could happen by the redistribution of the top Si layer while depositing metallic atoms, such as Au, Ag, and Sb, on the surface [32–34].

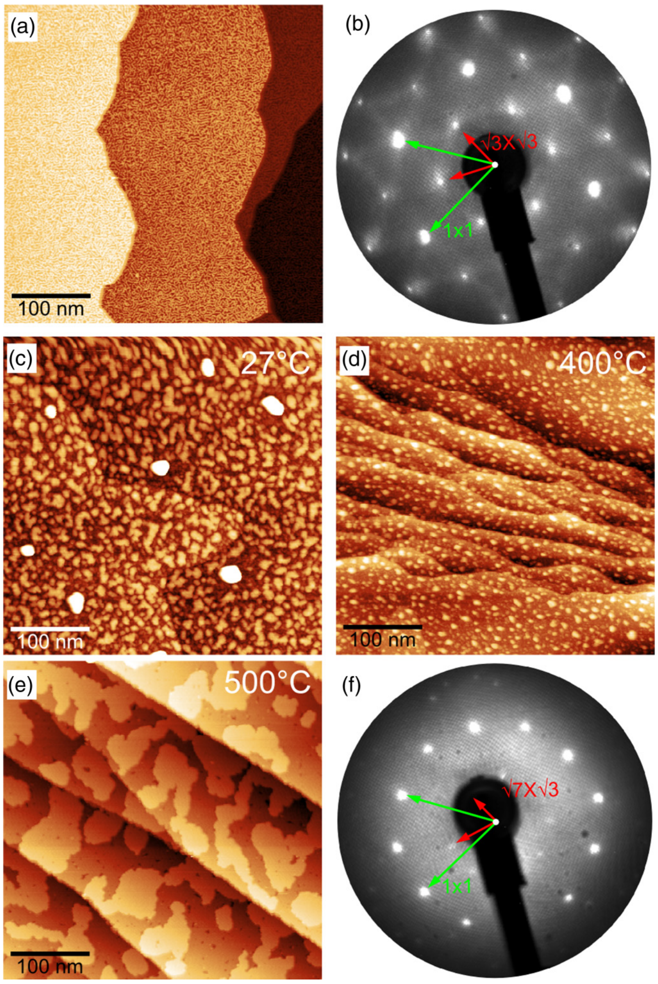

FIG. 1. (Color online) (a) $400 \times 400\,\text{nm}^2$ STM images of the Si(111)-α-$\sqrt{3}$-Au surface. (b) The LEED pattern of the Si(111)-α-$\sqrt{3}$-Au surface. (c)–(e) $400 \times 400\,\text{nm}^2$ STM images of 1.2 ML In on the Si(111)-α-$\sqrt{3}$-Au surface as grown and followed with annealing at different temperatures. (c) As grown. (d) 400 °C for 3 min. (e) 500 °C for 3 min. (f) The LEED pattern of (e). The LEED patterns were taken at 90 eV.

The structure of the $\sqrt{7}\times\sqrt{3}$ In overlayer was further confirmed by the atomically resolved STM. Two of the three $\sqrt{7}\times\sqrt{3}$ domains were observed with an angle of 120°, as shown in Fig. 2(a). This is compatible with the structure concluded from the LEED image shown in Fig. 1(f). The detailed analysis with zoomed in images at different sample biases (+0.7 V and +1.0 V) reveals the detailed insight on the surface structures, as depicted in Figs. 2(b) and 2(c). On both images, a clear $\sqrt{7}\times\sqrt{3}$ structure was observed. Nevertheless, not all the atoms observed in Fig. 2(c) are clearly visible in Fig. 2(b), illustrating that the contrasts which represent the atoms are bias dependent. Two types of atoms are distinct: one is for those clearly visible while the sample is biased at both +1.0 V and +0.7 V, and denoted by the blue dashed circles; the other is for those visible at +1.0 V but less contrasted at +0.7 V, and denoted by the white dashed circles. By measuring the height difference between the two types of atoms, it was found to be 0.18 Å at +0.7 V and 0.08 Å at +1.0 V. This indicates a strong LDOS inhomogeneity between the two types of atoms. The LDOS inhomogeneity is further observed on the dI/dV images which reflect only the LDOS, as shown in Figs. 2(d) and 2(e). At both sample biases, the dI/dV images show a brighter contrast at the type II atoms than at the type I atoms. On the other hand, a relatively similar contrast was observed for the same type of atoms. The LDOS inhomogeneity observed on both the topography and dI/dV images suggests that the two types of atoms have different underlying atomic configurations. Further results will be discussed in the DFT calculations.

Beyond the structure characterization, the In coverage of the structure can be identified by the atomically resolved

STM images. According to the image shown in Fig. 2(c), the In coverage corresponds to the 0.8 ML on the surface compared to the Si(111) atomic density. This is less than the 1.2 ML In coverage originally deposited at RT. The missing 0.4 ML of In was attributed to the desorption of In from the surface during the postannealing procedure at 500 °C, which is close to the desorption temperature 600 °C of In on the α-$\sqrt{3}$-Au surface [12,13]. This is a structure of In (0.8 ML with $\sqrt{7} \times \sqrt{3}$ superstructure) which has neither been found in the previous experiments nor been proposed in the DFT calculations [12,14].

It is noted that the surface we observed is not the Si(111)-$\sqrt{7} \times \sqrt{3}$-In surface in spite of its many similarities according to the LEED patterns and STM images [35,36]. Typically, the structure of In/Si(111) varies significantly with the measuring temperature [37]. The surface exhibits the $\sqrt{7} \times \sqrt{3}$ superstructure at RT, and undergoes a phase transition to $\sqrt{7} \times \sqrt{7}$ at temperatures below 200 K [37]. This is not the case in our observations. We found only one $\sqrt{7} \times \sqrt{3}$ phase at RT and at 78 K in the LEED pattern and in the STM images. Therefore, the observed $\sqrt{7} \times \sqrt{3}$ phase does not correspond to the In/Si(111) structure, which can rule out the possibility of In in contact with Si(111).

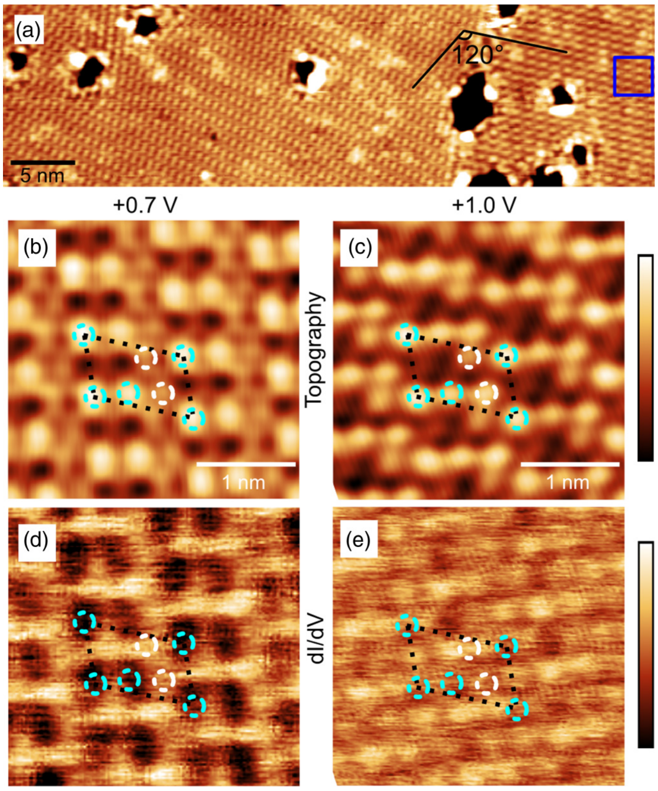

FIG. 2. (Color online) Atomically resolved surface taken by STM. (a) Two of the three $\sqrt{7} \times \sqrt{3}$ domains for In on Si(111)-α-$\sqrt{3}$-Au deviate with an included angle at 120°. The STM image was taken at sample bias +1.0 V. (b) and (c) are the multibias images taken at the area marked by the blue square in (a). The sample biases for the multibias images are +0.7 V and +1.0 V for the left and right images, respectively. The black dashed square is the unit cell of the $\sqrt{7} \times \sqrt{3}$ structure. The blue dashed circles mark the type I atoms and the white dashed circles mark the type II atoms. (d) and (e) are the dI/dV images for (b) and (c), respectively.

Another question one might ask is whether this $\sqrt{7} \times \sqrt{3}$ phase we observed is composed of a Au-In surface alloy. From the previous DFT results, the intermixing between In and Au on Si(111) is energetically unfavorable [14]. To intermix the In with Au to form the Au-In alloy, one has to prepare In directly on the Si(111) surface, then follow with the Au deposition [38]. The In adsorbed Si(111)-α-$\sqrt{3}$-Au structure was also confirmed by the angle-resolved photoemission spectroscopy. The spectra reveal that depositing In on Si(111)-α-$\sqrt{3}$-Au followed by annealing (at 600 °C) preserves the original CHCT structure [13]. All of these results indicate that the Au atoms do not prefer to form an alloy with In atoms. Therefore, the obtained $\sqrt{7} \times \sqrt{3}$ structure is believed to be an In surface structure and not a Au-In alloy.

As mentioned, the In coverage on the surface is 0.8 ML from the atomically resolved STM images. The STM images, however, give no clear relative atomic arrangement of the In atoms with the underlying Si(111)-α-$\sqrt{3}$-Au. To clarify the underlying structure, the DFT calculations were performed. In the calculation, we constructed a $\sqrt{7} \times \sqrt{3}$ unit cell based on the observation by LEED and atomic resolved STM. This unit cell has one basis vector the same as $\sqrt{3} \times \sqrt{3}$, and the other deviated by rotating 10.9° and further extending to $\sqrt{7}$ in length, as shown in Fig. 4(a). There are five Au atoms in this $\sqrt{7} \times \sqrt{3}$ unit cell in which the Au atoms are redistributed to the new positions. These positions are all close to the hollow sites of the Si surface but deviated from the center. The area density of Au in the $\sqrt{7} \times \sqrt{3}$ unit cell is the same as the CHCT model, which means the same Au coverages in both models (1 ML). The Si atoms underneath Au are around the T1 sites, while three of them form a trimer. Similarly, five possible positions of indium can be filled on this model. The proposed 0.8 ML was relaxed by introducing four In atoms with the experimental STM images as their initial geometries. The In structure was also determined by examining the relative surface energies at different In coverage: from 0.6 ML to 1.2 ML for the single-layered models. The lowest-energy model was further tested by shifting the In atoms in 54 different positions along the substrate. See Supplemental Material [39]. To confirm our results of the single-layered model, we also calculated the possible double-layered model from 1.6 ML to 2.4 ML. Based on the previous LEED and atomic STM images, two possible In structures, hexagonal and rectangular, were calculated [35,36,40]. For the single-layered models, the structure with 0.8 ML coverage is not only the lowest energy surface but also the only coverage which is energetically favorable over the CHCT Au structure. On the other hand, all of the double-layered models are of higher surface energies than the CHCT Au structure. The best fit model within all the examined double-layered models, in which the simulated STM image is comparable to the experimental one, is the 1.8 ML model. Figure 3 illustrates the comparison between the STM/STS measurements and the DFT calculations. The simulated STM images of both the 1.8 ML and the 0.8 ML models are similar to each other, as shown in the inset of Fig. 3. Nevertheless, their calculated LDOS as a function of energy look significantly different. The blue curve representing the LDOS for 0.8 ML shows a peak at around −0.85 eV, a right shoulder at −0.6 eV, three peaks at the energy between −0.2 eV and +0.5 eV, and a peak at around +1.0 eV. These

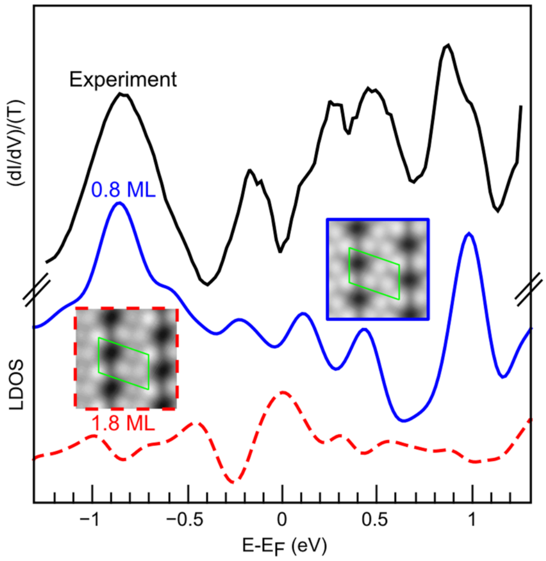

FIG. 3. (Color online) Normalized dI/dV spectrum (black line) and calculated LDOS of 0.8 ML (blue line) and 1.8 ML (red dashed line) In models. The simulated STM images of the models are shown in the inset. The normalized dI/dV spectrum is averaged from spectra at five different positions on the surface. The calculated LDOS were shifted upward +0.6 V in order to compare them with the measured dI/dV spectrum.

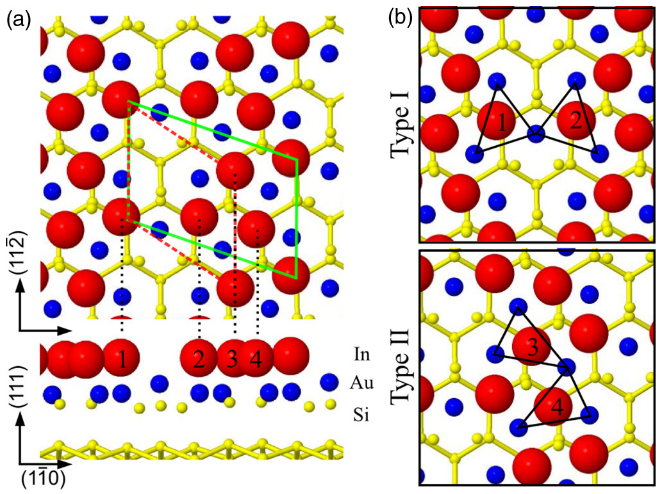

FIG. 4. (Color online) (a) Top view and side view of the proposed 0.8 ML In model from the DFT calculation. The red dashed line marks the $\sqrt{3} \times \sqrt{3}$ unit cell and the green line marks the $\sqrt{7} \times \sqrt{3}$ unit cell. Four different atoms with different atomic configurations are marked by 1 to 4. (b) Zoomed images of type I and type II atoms.

characteristics are very close to what we observed from the STS measurements (the black curve in Fig. 3). By contrast, the LDOS for 1.8 ML is significantly different from the experimental results. It is clear that the LDOS of the 0.8 ML model gives a better match with the experimental spectra. Moreover, the calculated 0.8 ML model fits better for the experimental structure on their atomic height. The corrugation of the In atoms in the calculated model is 0.09 Å, which is similar to our STM results (0.08–0.18 Å). On the other hand, the atomic structure of the double layered In gives a higher corrugation (0.3 Å) than the 0.8 ML model and that of the experiment. The In interlayer distance of the double-layered model is around 2.2 Å which is also not comparable to the 3.16 Å from the experiment. Therefore, by comparing the DFT calculations with the experiments, the observed surface is again confirmed to be 0.8 ML In coverage.

Finally, Fig. 4(a) shows the atomic configuration of the proposed 0.8 ML model. The In-Au interlayer distance in the model is 1.5–2.0 Å which is comparable to 1.8 Å in the previous results with lower In coverage [12]. Two different types of In atoms observed in STM are marked in the proposed model, as shown in Fig. 4(b). Even when all of the In atoms are surrounded by three Au atoms, it is still clear that they are in different atomic configurations. The type I atoms, marked as atoms 1 and 2, have symmetric Au trimmers underneath and a mirror symmetry along the [11$\bar{2}$] direction between the Au trimmers. On the other hand, the type II atoms, marked as atoms 3 and 4, have relatively asymmetric Au trimmers. Moreover, the closest In-Au distance of the type I atoms is shorter (∼2.5%) than that of the type II atoms. It results in stronger In-Au bonding (∼5%) for type I atoms and more charge transfer from the type I atoms to the underlying Au. The different charge transfer further changes the LDOS between the atoms [41,42]. This explains the observed LDOS inhomogeneity between the two types of atoms in the topography and dI/dV images.

IV. SUMMARY

In summary, we have found a surface structure with higher In coverage on Si(111)-α-$\sqrt{3}$-Au by depositing 1.2 ML In on top followed by annealing at 500 °C. A $\sqrt{7} \times \sqrt{3}$ structure with 0.8 ML In coverage was observed by STM and LEED, which has neither been observed in the previous experiments nor in the calculations. By the atomically resolved STM image and dI/dV image, the atomic structure of the $\sqrt{7} \times \sqrt{3}$ phase was studied and further compared with the DFT calculations. Both the simulated STM image and calculated LDOS of the 0.8 ML model agree well with the experimental results. From the STM images, two types of In atoms were observed which have LDOS inhomogeneity between them. The detailed atomic structure shows that the two types of In atoms have different atomic configurations underneath and different In-Au bond lengths. This results in the different charge transfers between the atoms and explains the observed LDOS inhomogeneity. As the In atoms were proposed to be electron doping [13,43], the extra In atoms of the 0.8 ML In structure could be of interest to study the change of electronic structure compared to the previous stable 0.15 ML In structure.

---

[1] S. Hasegawa, X. Tong, S. Takeda, N. Sato, and T. Nagao, Prog. Surf. Sci. **60**, 89 (1999).

[2] J. M. Carpinelli, H. H. Weitering, E. W. Plummer, and R. Stumpf, Nature (London) **381**, 398 (1996).

[3] H. W. Yeom, S. Takeda, E. Rotenberg, I. Matsuda, K. Horikoshi, J. Schaefer, C. M. Lee, S. D. Kevan, T. Ohta, T. Nagao, and S. Hasegawa, Phys. Rev. Lett. **82**, 4898 (1999).
[4] R. Cortés, A. Tejeda, J. Lobo, C. Didiot, B. Kierren, D. Malterre, E. G. Michel, and A. Mascaraque, Phys. Rev. Lett. **96**, 126103 (2006).
[5] W. H. Choi, P. G. Kang, K. D. Ryang, and H. W. Yeom, Phys. Rev. Lett. **100**, 126801 (2008).
[6] S. Qin, J. Kim, Q. Niu, and C.-K. Shih, Science **324**, 1314 (2009).
[7] K. S. Kim, S. C. Jung, M. H. Kang, and H. W. Yeom, Phys. Rev. Lett. **104**, 246803 (2010).
[8] S. D. Stolwijk, A. B. Schmidt, M. Donath, K. Sakamoto, and P. Krüger, Phys. Rev. Lett. **111**, 176402 (2013).
[9] H. M. Zhang, T. Balasubramanian, and R. I. G. Uhrberg, Phys. Rev. B **65**, 035314 (2001).
[10] H. M. Zhang, T. Balasubramanian, and R. I. G. Uhrberg, Phys. Rev. B **66**, 165402 (2002).
[11] J. N. Crain, K. N. Altmann, C. Bromberger, and F. J. Himpsel, Phys. Rev. B **66**, 205302 (2002).
[12] D. V. Gruznev, I. N. Filippov, D. A. Olyanich, D. N. Chubenko, I. A. Kuyanov, A. A. Saranin, A. V. Zotov, and V. G. Lifshits, Phys. Rev. B **73**, 115335 (2006).
[13] J. K. Kim, K. S. Kim, J. L. McChesney, E. Rotenberg, H. N. Hwang, C. C. Hwang, and H. W. Yeom, Phys. Rev. B **80**, 075312 (2009).
[14] C. H. Hsu, W. H. Lin, V. Ozolins, and F. C. Chuang, Phys. Rev. B **85**, 155401 (2012).
[15] T. Zhang, P. Cheng, W.-J. Li, Y.-J. Sun, G. Wang, X.-G. Zhu, K. He, L. Wang, X. Ma, X. Chen, Y. Wang, Y. Liu, H.-Q. Lin, J.-F. Jia, and Q.-K. Xue, Nat. Phys. **6**, 104 (2010).
[16] T. Uchihashi, P. Mishra, M. Aono, and T. Nakayama, Phys. Rev. Lett. **107**, 207001 (2011).
[17] M. Yamada, T. Hirahara, and S. Hasegawa, Phys. Rev. Lett. **110**, 237001 (2013).
[18] A. Saranin, A. Zotov, T. Numata, O. Kubo, K. Ignatovich, V. Lifshits, M. Katayama, and K. Oura, Surf. Sci. **388**, 299 (1997).
[19] S. Takeda, X. Tong, S. Ino, and S. Hasegawa, Surf. Sci. **415**, 264 (1998).
[20] T. Nagao, S. Hasegawa, K. Tsuchie, S. Ino, C. Voges, G. Klos, H. Pfnur, and M. Henzler, Phys. Rev. B **57**, 10100 (1998).
[21] V. A. Ukraintsev, Phys. Rev. B **53**, 11176 (1996).
[22] J. P. Perdew, K. Burke, and M. Ernzerhof, Phys. Rev. Lett. **77**, 3865 (1996).
[23] P. Hohenberg and W. Kohn, Phys. Rev. **136**, B864 (1964).
[24] W. Kohn and L. J. Sham, Phys. Rev. **140**, A1133 (1965).
[25] G. Kresse and D. Joubert, Phys. Rev. B **59**, 1758 (1999).
[26] G. Kresse and J. Hafner, Phys. Rev. B **47**, 558 (1993).
[27] G. Kresse and J. Furthmuller, Phys. Rev. B **54**, 11169 (1996).
[28] J. Tersoff and D. R. Hamann, Phys. Rev. B **31**, 805 (1985).
[29] J. Nogami, A. A. Baski, and C. F. Quate, Phys. Rev. Lett. **65**, 1611 (1990).
[30] J. Falta, A. Hille, D. Novikov, G. Materlik, L. Seehofer, G. Falkenberg, and R. Johnson, Surf. Sci. **330**, L673 (1995).
[31] K. Hermann and M. A. van Hove, http://www.fhi-berlin.mpg.de/KHsoftware/LEEDpat/index.html.
[32] A. Shibata, Y. Kimura, and K. Takayanagi, Surf. Sci. **273**, L430 (1992).
[33] R. G. Ryland, S. Hasegawa, and E. D. Williams, Surf. Sci. **345**, 222 (1996).
[34] A. Saranin, A. Zotov, V. Lifshits, J.-T. Ryu, O. Kubo, H. Tani, T. Harada, M. Katayama, and K. Oura, Surf. Sci. **429**, 127 (1999).
[35] J. Kraft, S. Surnev, and F. Netzer, Surf. Sci. **340**, 36 (1995).
[36] J. Kraft, M. G. Ramsey, and F. P. Netzer, Phys. Rev. B **55**, 5384 (1997).
[37] A. A. Saranin, A. V. Zotov, M. Kishida, Y. Murata, S. Honda, M. Katayama, K. Oura, D. V. Gruznev, A. Visikovskiy, and H. Tochihara, Phys. Rev. B **74**, 035436 (2006).
[38] D. Gruznev, A. Matetskiy, L. Bondarenko, E. Borisenko, D. Tsukanov, A. Zotov, and A. Saranin, Surf. Sci. **605**, 1420 (2011).
[39] See Supplemental Material at http://link.aps.org/supplemental/10.1103/PhysRevB.90.235407 for the coordinates of surface structure at 0.8 ML.
[40] K. Uchida and A. Oshiyama, Phys. Rev. B **87**, 165433 (2013).
[41] Z.-C. Dong, D. Fujita, and H. Nejoh, Phys. Rev. B **63**, 115402 (2001).
[42] P. Sobotik, M. Setvin, P. Zimmermann, P. Kocan, I. Ostadal, P. Mutombo, M. Ondracek, and P. Jelinek, Phys. Rev. B **88**, 205406 (2013).
[43] L. V. Bondarenko, D. V. Gruznev, A. A. Yakovlev, A. Y. Tupchaya, D. Usachov, O. Vilkov, A. Fedorov, D. V. Vyalikh, S. V. Eremeev, E. V. Chulkov, A. V. Zotov, and A. A. Saranin, Sci. Rep. **3**, 1826 (2013).